

# Quasiperiodic Van der Waals Heterostructures of Graphene and Hexagonal Boron Nitride

Sumanta Bhandary, Soumyajyoti Haldar, and Biplab Sanyal\*

**Advancement toward opening a bandgap at the Dirac point induced by symmetry breaking paved the way to realize 2D heterostructures with graphene and hexagonal boron nitride (h-BN). An alternate arrangement of graphene and h-BN layers in a 3D stacking can tune the bandgaps of these composites depending on the position of B and N atoms with respect to C atoms of graphene. Herein, a unique possibility of arranging graphene and h-BN atomic layers in a quasiperiodic Fibonacci sequence to study the possibilities of controlling the electronic properties of these heterostructures is explored. Density functional theory calculations combined with van der Waals corrections reveal that these quasiperiodic heterostructures are more stable than normal periodic stacking of monolayers of graphene and h-BN. Moreover, for certain arrangements of atomic layers, sizeable bandgaps can be obtained.**

## 1. Introduction

The discovery of 2D materials is extremely exciting because of their unique properties, resulting from the lowering of dimensionality. The experimental realization of graphene, an atomically thin 2D allotrope of carbon, by Geim et al.<sup>[1,2]</sup> made an enormous sensation owing to its exciting fundamental properties. Also, the apparent contradiction of the thermodynamic stability of this 2D material at a finite temperature<sup>[3,4]</sup> was found to be caused by the out-of-plane thermal distortion comparable to its

bond length.<sup>[5]</sup> An infinite 2D sheet of pristine graphene is a semimetal, i.e., a metal with zero bandgap. The inversion symmetry provided by  $P6/mmm$  space group results in the band degeneracy at the Dirac ( $K$ ) point in the hexagonal Brillouin zone (BZ). This limits its most anticipated application in electronics as the on-off current ratio for transistor applications becomes too small. Therefore, the opening of a bandgap is essential from electronics point of view retaining its high carrier mobility. Several approaches have been already considered by modifying graphene either chemically<sup>[6–8]</sup> or by structural confinement<sup>[9,10]</sup> to improve its application possibilities.

Boron nitride, on the other hand, can have different forms of structures such


as bulk hexagonal boron nitride (h-BN) with  $sp^2$  bond and cubic boron nitride with  $sp^3$  bond, analogous to graphite and diamond, respectively. A 2D form of h-BN with strong  $sp^2$  bond can also be experimentally synthesized, which resembles its carbon counterpart, graphene. In contrast to graphene, two different atomic species in two sublattices forbid the inversion symmetry, which results in the lifting of band degeneracy at Dirac point in BZ, and hence gives rise to an insulating bandgap of 5.97 eV.<sup>[11]</sup>

A new horizon opens up with a different class of materials composed of these neighboring elements in the periodic table. The first possibility is to alloy graphene and h-BN to form another group of 2D materials. B–N bond length is just 1.7% larger than C–C bond, which makes them perfect for alloying with minimal internal stress.<sup>[6,12–14]</sup> At the same time, the introduction of h-BN in graphene breaks the inversion symmetry which can open up a bandgap in graphene. On top of that, the Pauling electronegativity of B, C, and N are 2.04, 2.55, and 3.04, respectively, indicating that the charge transfer in different kinds of hybrid heterostructures of graphene and h-BN may play an interesting role in both stability and electronic properties. The other possibility is to form van der Waals (vdW) heterostructures by stacking graphene and h-BN layers in a different fashion. Depending on how the h-BN layer is placed on top of a graphene layer, sublattice degeneracy will be affected. A controlled growth process can thus provide the tunability of bandgap opening in graphene and h-BN heterostructures. In recent years, heterostructures formed by graphene and h-BN have gained extensive attention.<sup>[15–21]</sup> Moire patterns discovered in this slightly lattice-mismatched superlattice and also slightly rotated bilayer graphene (BLG) have given rise to several exotic phenomena, such as superconductivity,<sup>[22]</sup> fractional Chern insulating states, magnetism,<sup>[23]</sup> and so on and ample scope of tunability.<sup>[24]</sup>

S. Bhandary  
School of Physics and CRANN Institute  
Trinity College Dublin  
The University of Dublin  
Dublin 2, Ireland

S. Haldar  
Institute of Theoretical Physics and Astrophysics  
University of Kiel  
Leibnizstrasse 15, 24098 Kiel, Germany

B. Sanyal  
Department of Physics and Astronomy  
Uppsala University  
Box-516, SE 75120, Sweden  
E-mail: Biplab.Sanyal@physics.uu.se

 The ORCID identification number(s) for the author(s) of this article can be found under <https://doi.org/10.1002/pssb.202100423>.

© 2021 The Authors. physica status solidi (b) basic solid state physics published by Wiley-VCH GmbH. This is an open access article under the terms of the Creative Commons Attribution License, which permits use, distribution and reproduction in any medium, provided the original work is properly cited.

DOI: 10.1002/pssb.202100423

High mobility and a large spin lifetime have been realized in graphene spintronics<sup>[25]</sup> by using layered h-BN as a substrate. Recently, the importance of Rashba spin-orbit coupling and spin relaxation properties has been highlighted<sup>[26]</sup> theoretically for graphene/h-BN heterostructures.

So far, the normal periodic stacking of graphene and h-BN has been considered as models of 3D hybrid heterostructures. Recent experiments have shown that the vertical graphene heterostructures with h-BN or molybdenum disulfide (MoS<sub>2</sub>) can work as field-effect tunneling transistors.<sup>[15,27]</sup> Tuning of bandgap is also possible using BLG h-BN heterostructures.<sup>[28]</sup> Bipolar doping of double-layer graphene with hydrogenated BN has also been studied, where it has been shown that by tuning the interlayer distance, the interfacial dipole and screening charge distribution can be significantly affected.<sup>[29]</sup> Low-loss plasmon damping has also been observed in graphene h-BN heterostructures, which can be key to nanophotonic and nano-optoelectronic devices.<sup>[30,31]</sup> In these heterostructures, it is also possible to tune the optical conductivity of graphene in the visible range and obtain optical excitations that are not present in the individual building blocks.<sup>[32–34]</sup> The stacking has a strong impact on the spatial distribution and the character of the generated electron-hole pairs.<sup>[34–36]</sup> Bandgaps of these 3D heterostructures can also be modified using an external electric field.<sup>[37]</sup> Ferromagnetic junctions with these kinds of heterostructures are also gaining interest in the field of spintronics devices.<sup>[38]</sup> However, there are not any studies on quasiperiodic 3D stacking of graphene and h-BN monolayers.

Therefore, in this article, we aim to explore the possibilities of breaking sublattice degeneracies in quasiperiodic heterostructures. In this article, we have considered a quasiperiodic 3D stacking of 2D graphene and h-BN monolayers in a Fibonacci sequence. The Fibonacci quasicrystal has exotic spectral features such as critical eigenfunctions, a spectrum with zero measure, and unique scaling behavior.<sup>[39–41]</sup> Binary layered structures have been synthesized in a Fibonacci sequence in one direction keeping pure translation periodicity in other directions. SiO<sub>2</sub> and TiO<sub>2</sub> dielectric slabs arranged in Fibonacci order have been grown<sup>[42]</sup> to verify the theoretical prediction<sup>[43]</sup> of localization of light in Fibonacci dielectric multilayers. Metallic Fibonacci multilayers were grown, and superconductivity was experimentally studied by Kartkut et al. using MoV superlattices.<sup>[44]</sup> In this work, we have studied structural and electronic properties of 3D Fibonacci heterostructures of graphene and h-BN to explore the possibilities of bandgap opening and stability of quasiperiodically arranged atomic layers using first-principles electronic structure calculations.

## 2. Results and Discussion

### 2.1. Structural Information

It has been shown theoretically that a graphene layer deposited on an h-BN substrate induces a bandgap opening in graphene.<sup>[45]</sup> This has been followed by several works, where a graphene monolayer or a bilayer sandwiched between the h-BN layer is studied. In these structures, the graphene layer is protected by h-BN apart from forming C–N, C–B out-of-plane dipoles. Formation of this dipole and its position with respect to two C-sublattices define the  $\pi - \pi^*$  band degeneracy breaking at the Dirac points. A similar approach,

like opening up a bandgap in BLG with applied electric field, is also seen to tune the bandgap in these kinds of systems.<sup>[46,47]</sup>

In our proposed superlattices, h-BN and graphene layers occur in a Fibonacci sequence,  $S_j$ , following a recurrence relation:  $S_{j+1} = \{S_j, S_{j-1}\}$ ,  $S_0 = \{B\}$ , and  $S_1 = \{A\}$ . A and B correspond to graphene and h-BN single layers, respectively. With this approach, the first few sequences of Fibonacci will be  $S_2 = \{AB\}$ ,  $S_3 = \{ABA\}$ , and  $S_4 = \{ABAAB\}$ . **Figure 1** shows a schematic representation of this quasiperiodic sequence. We followed the Bernal stacking for the arrangement of the individual layers. Being limited by the computational feasibility, we have considered finite-sized Fibonacci heterostructures with 13, 21, 34, and 55 layers with the number of BN layers ( $N_{BN}$ ) and the number of graphene layers ( $N_C$ ) to be (5, 8), (8, 13), (13, 21), and (21, 34), respectively. By swapping the composition, reverse structures are also obtained with the number of  $N_{BN}$  and  $N_C$  layers as (8, 5), (13, 8), (21, 13), and (34, 21), respectively. The swapping has a twofold impact: 1) the concentration of C and h-BN layers changes and 2) the interface ordering also varies, although the number of interfaces remains the same.

To achieve the golden ratio (two quantities are in the golden ratio if their ratio is the same as the ratio of their sum to the larger of the two quantities. It is an irrational number with a value of  $\varphi = \frac{1+\sqrt{5}}{2}$ ) with the number of graphene and h-BN layers, one should have an infinitely long sequence of Fibonacci ordering. For computational limitations, we have gone up to 55 atomic layers (110 atoms) in the unit cell. To be precise, we have considered the following atomic arrangements of different sequences: 1) 5 h-BN and 8 graphene, 2) 8 h-BN and 13 graphene, 3) 13 h-BN and 21 graphene, and 4) 21 h-BN and 34 graphene layers in the unit cells, referred to as the forward direction. Henceforth, these structures are referred to as Fib13, Fib21, Fib34, and Fib55, respectively. The same nomenclatures have been used for the *reverse* direction, where graphene (h-BN) layers are replaced by h-BN (graphene) layers. For the completeness of the study, we have also considered superlattices having regular periodic stacking with h-BN graphene ratios 1:1, 2:1, 3:1, 4:1, 5:1, and 1:1 with a bilayer stacking. This study may

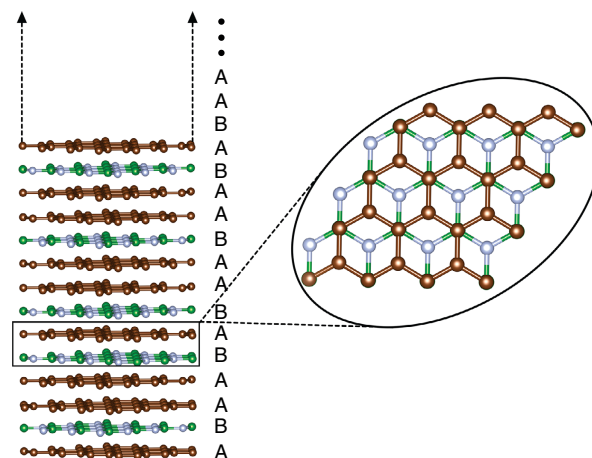


**Figure 1.** Schematic representation of Fibonacci stacking of graphene and hexagonal boron-nitride sequence. Inset shows the schematic representation of Bernal stacking which is used to form Fibonacci structures.



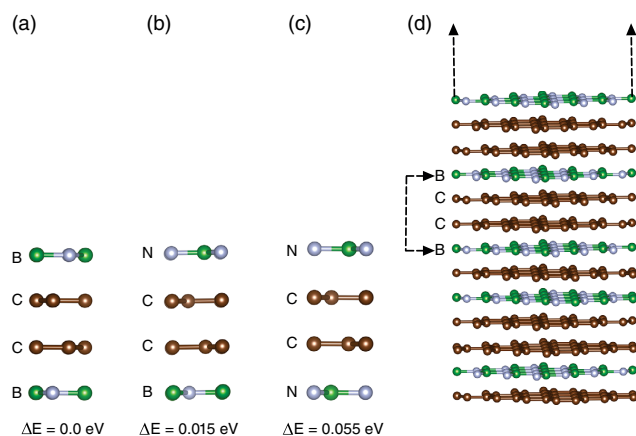


**Figure 3.** Schematic representation of different building blocks (a-c) of Fibonacci stacking and their relative formation energy. Here the layers are in Bernal (AB) stacking. Therefore, three possible different stacking can be achieved along the  $c$  axis, namely a) B-C-C-B, b) B-C-C-N, and c) N-C-C-N. Figure 3d shows the Fibonacci stacking of graphene and h-BN with most stable building block (B-C-C-B) in it.

of the layers, three possible different stacking for the building blocks can be achieved along the  $c$  axis. These blocks are 1) B-C-C-B, 2) B-C-C-N, and 3) N-C-C-N (see Figure 3a-c). The formation energy analysis indicates that the B-C-C-B structure is energetically most probable among the others. However, from the literature, it is known that the B-C-C-N sequence can only open up a bandgap.<sup>[28]</sup> One thing to note here is that in B-C-C-N configurations, the layers are in AB stacking and the two C atoms belong to two different sublattices of two different graphene layers. These two situations of single-layer graphene and BLG are building blocks for our Fibonacci superlattices. As we have AB stacking in the Fibonacci stacking and have always similar h-BN layers (i.e., all h-BN layers have B atom as sublattice A and N atom as sublattice B), single-layer graphene will always have the B-C-B situation, while a BLG will have only B-C-C-B configuration, which are semiconducting and metallic blocks, respectively. So, as a whole, we got metallic situations for the forward structures, no matter how many layers we have considered.

## 2.2. Energetics

Table 2 shows the formation energies of these multilayered structures for both forward and reverse (in parentheses) directions. From the data presented in the table, we can conclude that it is possible to stabilize these quasiperiodic structures from 2D graphene and h-BN layers. To check the stability of these quasiperiodically stacked heterostructures as compared to the corresponding normal multilayer periodic stacking, we have also compared the formation energies of these two kinds of systems. Our calculations revealed that formation energies of the quasiperiodic structures are quite lower than the corresponding normal multilayer structure (see Table 2). From the analysis of energetics, we also found that the reverse structures are more stable than the forward structures, only visible after the inclusion of vdW interactions.

**Table 2.** Formation energy  $E_f$ /interface (in meV) of the hybrid structures calculated within LDA and PBE-vdW methods. For interfaces, we have considered the number of h-BN and graphene interfaces only. The bandgaps,  $E_g$  (in meV), for the reverse structures within PBE-vdW formalism are also shown. The forward structures do not have any bandgap.

System	$E_f$ /interface		$E_g$
	LDA	PBE-vdW	
Fib13	-63 (-63)	-158 (-169)	13
Fib21	-65 (-65)	-161 (-172)	42
Fib34	-66 (-65)	-162 (-173)	25
Fib55	-66 (-66)	- (-171)	-
BNC 1:1	-51	-130	-

## 2.3. Electronic Structure

In Table 2, we have tabulated the bandgaps of Fib13, Fib21, and Fib34 reverse quasiperiodic structures as obtained using the PBE-vdW method. It is seen that for Fib21 reverse structure, we find the maximum value of the bandgap. An oscillation in the values of the bandgaps is observed. This is related to the quasiperiodic behavior of the heterostructures. A similar behavior was reported previously for quasiperiodic carbon-BN nanoribbons by Pedreira et al.<sup>[48]</sup> Figure 4a shows the band structure plots for the reverse quasiperiodic structure of Fib21 where a small bandgap opening at the Dirac point can be observed (see close-up view of Figure 4a). To find out the nature of orbital characteristics of the valence band maximum (VBM) and conduction band minimum (CBM) at Dirac point for reverse Fib21 structure, we have calculated the partial charge densities for VBM and CBM at the Dirac point. Figure 4b shows a schematic diagram of band level splitting in the Fib21 reverse structure along with the partial charge density plots for VBM and CBM at Dirac point.

## 3. Conclusion

In summary, we have studied 3D heterostructures of 2D layers of graphene and h-BN stacked in a quasiperiodic Fibonacci sequence by vdW corrected density functional theory. We demonstrate that this quasiperiodic arrangement is more stable than a normal 1:1 periodic arrangement of graphene and h-BN layers. The effect of adding vdW correction in the stability and interplanar separations is shown. Finally, we show that for certain arrangements of Fibonacci stacking, it is possible to open up bandgaps of the order of tens of meV at the Dirac point. We hope that our prediction will encourage the experimentalists to grow these quasiperiodic heterostructures.

## 4. Methods

All our first-principles calculations have been performed using a plane-wave basis within the density functional theory as implemented in the Vienna *ab initio* simulation package (VASP)



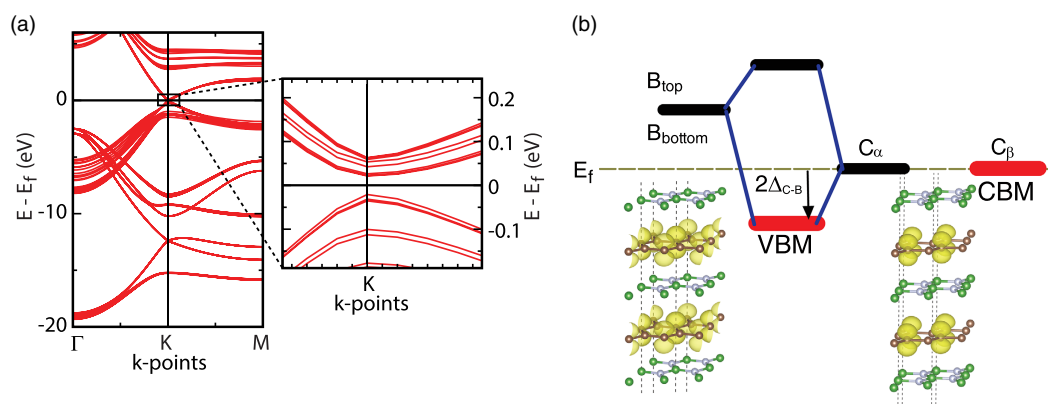


**Figure 4.** a) Band structure of Fib21 system with the reverse order of graphene and h-BN layers. The picture on the right side is a close-up of the band structure near the Fermi energy to show the opening of a bandgap at the Dirac point. b) Schematic diagram of band level splitting in Fib21 reverse structure along with the partial charge density plots for valence band maximum (VBA) and conduction band minimum (CBM) at Dirac point.

code.<sup>[49]</sup> An energy cutoff of 500 eV was used to expand the wave functions. Generalized gradient approximation as proposed by Perdew, Burke, and Ernzerhof (PBE)<sup>[50,51]</sup> has been used for the exchange-correlation functional. To describe the electron-ion interactions, we have used the projector augmented wave methods (PAW).<sup>[52,53]</sup> We have also included vdW interactions within the DFT-D2 formalism of Grimme (PBE + vdW)<sup>[54]</sup> to incorporate the interlayer interactions. Recent papers<sup>[55,56]</sup> have shown that the choice of vdW correction method is not significantly important for describing the properties of graphene and h-BN composites. Moreover, for comparison, we have also performed calculations with local density approximation (LDA) as it is known that in many cases, LDA can give rise to a reasonable agreement with the experimental results for vdW bonded systems.<sup>[57]</sup> The structures have been optimized using the conjugate gradient method with forces calculated from the Hellmann-Feynman theorem. We have used the force tolerance of  $0.01\text{ eV \AA}^{-1}$  along with the energy tolerance of  $10^{-5}$  eV for our calculations. For geometry optimizations, a  $15 \times 15 \times 2\Gamma$ -centered k-point mesh has been used for the full BZ integration. For density of states (DOS) calculations, we have used  $45 \times 45 \times 2\Gamma$ -centered k-point mesh.

The formation energy  $E_f$  of graphene/h-BN hybrid system is defined as follows

$$E_f = E(\text{Graphene}_m + \text{BN}_n) - [m \times E(\text{Graphene}) + n \times E(\text{BN})] \quad (1)$$

where  $E(\text{Graphene} + \text{BN})$  is the total energy of the hybrid graphene/h-BN system,  $E(\text{Graphene})$  is the total energy of a single-layer graphene, and  $E(\text{BN})$  is the total energy of a single-layer h-BN.  $m$  and  $n$  represent the number of graphene and h-BN layers, respectively.

## Acknowledgements

B.S. acknowledges Carl Tryggers Stiftelse (CTS 20:378) and Swedish Research Council (2017-05447) for financial support. The authors thank

SNIC-NSC and SNIC-HPC2N computing centers under Swedish National Infrastructure for Computing (SNIC) for granting computer time (project no. SNIC2020-3-26) and PRACE DECI-17 project Q2Dtopomat.

## Conflict of Interest

The authors declare no conflict of interest.

## Data Availability Statement

Research data are not shared.

## Keywords

computational physics, density functional theory, Fibonacci sequences, van der Waals heterostructures

Received: August 19, 2021

Revised: September 23, 2021

Published online: November 21, 2021

- [1] K. S. Novoselov, A. K. Geim, S. V. Morozov, D. Jiang, Y. Zhang, S. V. Dubonos, I. V. Grigorieva, A. A. Firsov, *Science* **2004**, *306*, 5696.
- [2] A. K. Geim, K. S. Novoselov, *Nat. Mater.* **2007**, *6*, 183.
- [3] R. E. Peierls, *Ann. I. H. Poincaré* **1935**, *5*, 177.
- [4] L. D. Landau, *Phys. Z. Sowjetunion* **1937**, *11*, 26.
- [5] A. Fasolino, J. H. Los, M. I. Katsnelson, *Nat. Mater.* **2007**, *6*, 858.
- [6] J. Zhu, S. Bhandary, B. Sanyal, H. Ottosson, *J. Phys. Chem. C* **2011**, *115*, 10264.
- [7] S. Halder, D. Kanhere, B. Sanyal, *Phys. Rev. B* **2012**, *85*, 155426.
- [8] P. Chandrachud, B. S. Pujari, S. Halder, B. Sanyal, D. G. Kanhere, *J. Phys.: Condens. Matter* **2010**, *22*, 465502.
- [9] S. Bhandary, O. Eriksson, B. Sanyal, M. Katsnelson, *Phys. Rev. B* **2010**, *82*, 165405.
- [10] S. Halder, S. Bhandary, S. Bhattacharjee, O. Eriksson, D. Kanhere, B. Sanyal, *Solid State Commun.* **2012**, *152*, 1719.
- [11] K. Watanabe, T. Taniguchi, H. Kanda, *Nat. Mater.* **2004**, *3*, 404.
- [12] S. Halder, P. Srivastava, O. Eriksson, P. Sen, B. Sanyal, *J. Phys. Chem. C* **2013**, *117*, 21763.

- [13] Z. Liu, L. Ma, G. Shi, W. Zhou, Y. Gong, S. Lei, X. Yang, J. Zhang, J. Yu, K. P. Hackenberg, A. Babakhani, J.-C. Idrobo, R. Vajtai, J. Lou, P. M. Ajayan, *Nat. Nanotechnol.* **2013**, 8, 119.
- [14] S. Bhowmick, A. K. Singh, B. I. Yakobson, *J. Phys. Chem. C* **2011**, 115, 9889.
- [15] L. Britnell, R. V. Gorbachev, R. Jalil, B. D. Belle, F. Schedin, A. Mishchenko, T. Georgiou, M. I. Katsnelson, L. Eaves, S. V. Morozov, N. M. R. Peres, J. Leist, A. K. Geim, K. S. Novoselov, L. A. Ponomarenko, *Science* **2012**, 335, 947.
- [16] L. Britnell, R. M. Ribeiro, A. Eckmann, R. Jalil, B. D. Belle, A. Mishchenko, Y.-J. Kim, R. V. Gorbachev, T. Georgiou, S. V. Morozov, A. N. Grigorenko, A. K. Geim, C. Casiraghi, A. H. C. Neto, K. S. Novoselov, *Science* **2013**, 340, 1311.
- [17] C. R. Woods, L. Britnell, A. Eckmann, R. S. Ma, J. C. Lu, H. M. Guo, X. Lin, G. L. Yu, Y. Cao, R. V. Gorbachev, A. V. Kretinin, J. Park, L. A. Ponomarenko, M. I. Katsnelson, Y. Gornostyrev, K. Watanabe, T. Taniguchi, C. Casiraghi, H.-J. Gao, A. K. Geim, K. S. Novoselov, *Nat. Phys.* **2014**, 10, 451.
- [18] A. Mishchenko, J. S. Tu, Y. Cao, R. V. Gorbachev, J. R. Wallbank, M. T. Greenaway, V. E. Morozov, S. V. Morozov, M. J. Zhu, S. L. Wong, F. Withers, C. R. Woods, Y.-J. Kim, K. Watanabe, T. Taniguchi, E. E. Vdovin, O. Makarovskiy, T. M. Fromhold, V. I. Fal'ko, A. K. Geim, L. Eaves, K. S. Novoselov, *Nat. Nanotechnol.* **2014**, 9, 808.
- [19] Q. Li, M. Liu, Y. Zhang, Z. Liu, *Small* **2016**, 12, 32.
- [20] D. Pierucci, J. Zribi, H. Henck, J. Chaste, M. G. Silly, F. Bertran, P. Le Fevre, B. Gil, A. Summerfield, P. H. Beton, S. V. Novikov, G. Cassaboiss, J. E. Rault, A. Ouerghi, *Appl. Phys. Lett.* **2018**, 112, 253102.
- [21] M. Yankowitz, Q. Ma, P. Jarillo-Herrero, B. J. LeRoy, *Nat. Rev. Phys.* **2019**, 1, 112.
- [22] Y. Cao, V. Fatemi, S. Fang, K. Watanabe, T. Taniguchi, E. Kaxiras, P. Jarillo-Herrero, *Nature* **2018**, 556, 43.
- [23] A. L. Sharpe, E. J. Fox, A. W. Barnard, J. Finney, K. Watanabe, T. Taniguchi, M. A. Kastner, D. Goldhaber-Gordon, *Science* **2019**, 365, 605.
- [24] N. R. Finney, M. Yankowitz, L. Muraleetharan, K. Watanabe, T. Taniguchi, C. R. Dean, J. Hone, *Nat. Nanotechnol.* **2019**, 14, 1029.
- [25] S. Roche, J. Åkerman, B. Beschoten, J.-C. Charlier, M. Chshiev, S. P. Dash, B. Dlubak, J. Fabian, A. Fert, M. Guimarães, F. Guinea, I. Grigorieva, C. Schönenberger, P. Seneor, C. Stampfer, S. O. Valenzuela, X. Waintal, B. van Wees, *2D Mater.* **2015**, 2, 030202.
- [26] K. Zollner, A. W. Cummings, S. Roche, J. Fabian, *Phys. Rev. B* **2021**, 103, 075129.
- [27] S. Kang, B. Fallahazad, K. Lee, H. Movva, K. Kim, C. Corbet, T. Taniguchi, K. Watanabe, L. Colombo, L. Register, E. Tutuc, S. Banerjee, *IEEE Electron Device Lett.* **2015**, 36, 405.
- [28] A. Ramasubramaniam, D. Naveh, E. Towe, *Nano Lett.* **2011**, 11, 1070.
- [29] Z. Liu, R.-Z. Wang, L.-M. Liu, W.-M. Lau, H. Yan, *Phys. Chem. Chem. Phys.* **2015**, 17, 11692.
- [30] A. Woessner, M. B. Lundeberg, Y. Gao, A. Principi, P. Alonso-González, M. Carrega, K. Watanabe, T. Taniguchi, G. Vignale, M. Polini, J. Hone, R. Hillenbrand, F. H. L. Koppens, *Nat. Mater.* **2015**, 14, 421.
- [31] A. Principi, M. Carrega, M. B. Lundeberg, A. Woessner, F. H. L. Koppens, G. Vignale, M. Polini, *Phys. Rev. B* **2014**, 90, 165408.
- [32] T. Stauber, N. M. R. Peres, A. K. Geim, *Phys. Rev. B* **2008**, 78, 085432.
- [33] G. J. Slotman, M. M. van Wijk, P.-L. Zhao, A. Fasolino, M. I. Katsnelson, S. Yuan, *Phys. Rev. Lett.* **2015**, 115, 186801.
- [34] W. Aggoune, C. Cocchi, D. Nabok, K. Rezouali, M. Akli Belkhir, C. Draxl, *J. Phys. Chem. Lett.* **2017**, 8, 1464.
- [35] W. Aggoune, C. Cocchi, D. Nabok, K. Rezouali, M. A. Belkhir, C. Draxl, *Phys. Rev. B* **2018**, 97, 241114.
- [36] W. Aggoune, C. Cocchi, D. Nabok, K. Rezouali, M. A. Belkhir, C. Draxl, *Phys. Rev. Mater.* **2020**, 4, 084001.
- [37] X. Zhong, R. G. Amorim, R. H. Scheicher, R. Pandey, S. P. Karna, *Nanoscale* **2012**, 4, 5490.
- [38] J.-F. Dayen, S. J. Ray, O. Karis, I. J. Vera-Marun, M. V. Kamalakar, *Appl. Phys. Rev.* **2020**, 7, 011303.
- [39] M. Kohmoto, L. P. Kadanoff, C. Tang, *Phys. Rev. Lett.* **1983**, 50, 1870.
- [40] S. Ostlund, R. Pandit, D. Rand, H. J. Schellnhuber, E. D. Siggia, *Phys. Rev. Lett.* **1983**, 50, 1873.
- [41] M. Kohmoto, B. Sutherland, C. Tang, *Phys. Rev. B* **1987**, 35, 1020.
- [42] W. Gellermann, M. Kohmoto, B. Sutherland, P. C. Taylor, *Phys. Rev. Lett.* **1994**, 72, 633.
- [43] M. Kohmoto, B. Sutherland, K. Iguchi, *Phys. Rev. Lett.* **1987**, 58, 2436.
- [44] M. G. Karkut, J. M. Triscone, D. Arios, O. Fischer, *Phys. Rev. B* **1986**, 34, 4390.
- [45] G. Giovannetti, P. A. Khomyakov, G. Brocks, P. J. Kelly, J. van den Brink, *Phys. Rev. B* **2007**, 76, 073103.
- [46] K. F. Mak, C. H. Lui, J. Shan, T. F. Heinz, *Phys. Rev. Lett.* **2009**, 102, 256405.
- [47] Y. Yamashiro, Y. Ohno, K. Maehashi, K. Inoue, K. Matsumoto, *J. Vac. Sci. Technol. B* **2012**, 30, 03D111.
- [48] D. O. Pedreira, S. Azevedo, C. G. Bezerra, A. Viol, G. M. Viswanathan, M. S. Ferreira, *Solid State Commun.* **2014**, 180, C 28.
- [49] G. Kresse, J. Furthmüller, *Phys. Rev. B* **1996**, 54, 11169.
- [50] J. P. Perdew, K. Burke, M. Ernzerhof, *Phys. Rev. Lett.* **1996**, 77, 3865.
- [51] J. P. Perdew, K. Burke, M. Ernzerhof, *Phys. Rev. Lett.* **1997**, 78, 1396.
- [52] P. E. Blöchl, *Phys. Rev. B* **1994**, 50, 17953.
- [53] G. Kresse, D. Joubert, *Phys. Rev. B* **1999**, 59, 1758.
- [54] S. Grimme, *J. Comput. Chem.* **2006**, 27, 1787.
- [55] X. Kong, L. Li, F. M. Peeters, *J. Phys.: Condens. Matter* **2019**, 31, 255302.
- [56] J. R. M. Sevilla, D. B. Putungan, *Mater. Res. Express* **2021**, 8, 085601.
- [57] I. Mosyagin, D. Gambino, D. G. Sangiovanni, I. A. Abrikosov, N. M. Caffrey, *Phys. Rev. B* **2018**, 98, 174103.